IEEE Access
Multidisciplinary : Rapid Review : Open Access Journal

Received March 5, 2019, accepted March 19, 2019, date of publication March 29, 2019, date of current version April 13, 2019.

Digital Object Identifier 10.1109/ACCESS.2019.2907749

Design of a Superstrate Module for Simple Resonant Frequency Tuning

TAE HEUNG LIM[1], HOSUNG CHOO[1], (Senior Member, IEEE), AND GANGIL BYUN[2], (Member, IEEE)
[1]School of Electronic and Electrical Engineering, Hongik University, Seoul 04066, South Korea
[2]School of Electrical and Computer Engineering, Ulsan National Institute of Science and Technology, Ulsan 44919, South Korea

Corresponding author: Gangil Byun (byun@unist.ac.kr)

This work was supported in part by the Research Fund of Signal Intelligence Research Center supervised by the Defense Acquisition Program Administration, Agency for Defense Development of Korea, and in part by the National Research Foundation of Korea (NRF) grant funded by the Korean Government (Basic Research) under Grant NRF-2017R1D1A1B04031890.

ABSTRACT This paper proposes the design of a dual-band circularly polarized antenna with an exchangeable superstrate module to compensate for the unwanted frequency shift without the re-fabrication process. The proposed antenna consists of inner and outer circular ring patches printed on the same layer of a substrate, and the mushroom-shaped superstrate is inserted to the substrate hole placed in the middle of the inner ring patch. The proposed superstrate structure adaptively adjusts the resonant frequency by selecting appropriate heights of the superstrate module. By inserting the superstrate module with the height of 2 mm, the maximum frequency shift of 20 MHz was obtained with the improved gain of about 0.9 dB at 1.42 GHz without any deteriorations on the AR and radiation patterns.

INDEX TERMS Dielectric substrate, antennas, frequency control, dielectric devices.

I. INTRODUCTION

Dual-band microstrip patch antennas with circular polarization (CP) have been widely adopted for global navigation satellite system (GNSS) and satellite digital audio radio service (SDARS) to maintain high reception reliability [1]–[3]. Current research trends for these applications are mainly focused on the miniaturization of antenna aperture since the given space for antennas is often limited to less than a quarter wavelength at a target frequency. Thus, there has been a tremendous effort to miniaturize the antenna size. The most common approach is the use of high permittivity materials for antenna substrates [4]–[6]. It is also well-known that the insertion of slots [7]–[9], shorting pins [10]–[12], or fractal geometries [13]–[15] are also popular miniaturization techniques. However, these techniques often produce narrow CP and impedance matching bandwidths that result in the increased frequency sensitivity. In other words, the antenna characteristics can be easily degraded by an unwanted frequency shift due to the existence of platform effects [16], mutual coupling [9], and fabrication error [17]. This performance degradation becomes more challenging for circularly polarized antennas whose AR and impedance matching bandwidths should be overlapped [18]–[21]. Although some papers reported good results on the reduced sensitivity using an electromagnetically coupled feed structure [22], [23] and an air gap structure without the substrate [24], [25], they still require an extra re-fabrication process for an undesired frequency shift.

In this paper, we propose the design of a single-layer dual-ring CP antenna with an exchangeable superstrate module that can compensate for the unexpected frequency shift of both the AR and the reflection coefficient without the re-fabrication process. The proposed antenna consists of inner and outer circular ring patches that are printed on a substrate, and the substrate has a cylindrical hole in the middle of the inner ring patch. The superstrate module has a mushroom shape to be inserted to the cylindrical hole for minimized offset error between centers of the superstrate module and the ring patches. Note that the head of the superstrate module has an identical diameter with the inner patch, and its thickness is varied to adjust the effective dielectric constant only for the upper resonance. To demonstrate the feasibility, we first derive formulations of the theoretical effective permittivity for a circular ring patch antenna based on the cavity model [26]. The derived formulations are provided as a function of permittivity and the superstrate thickness with an assumption that the substrate, superstrate, and ground layers

The associate editor coordinating the review of this manuscript and approving it for publication was Qingfeng Zhang.

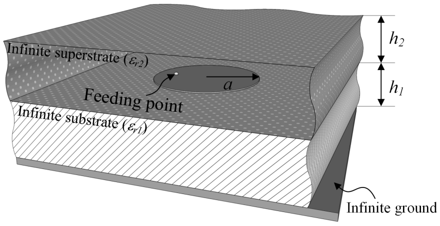

FIGURE 1. Conceptual geometry of the infinite superstrate patch antenna with the infinite ground.

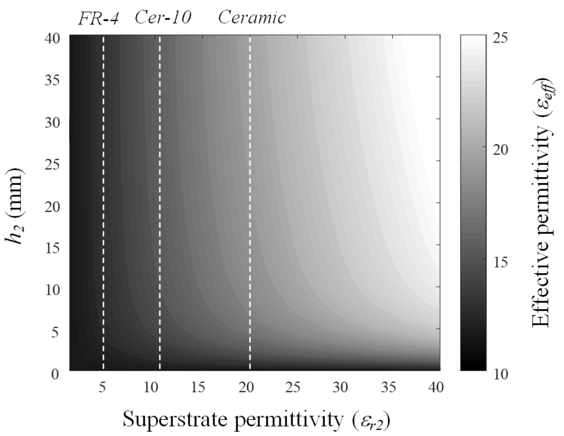

FIGURE 2. The effective permittivity of the ring patch antenna with the superstrate according to h_2 and ε_{r2}.

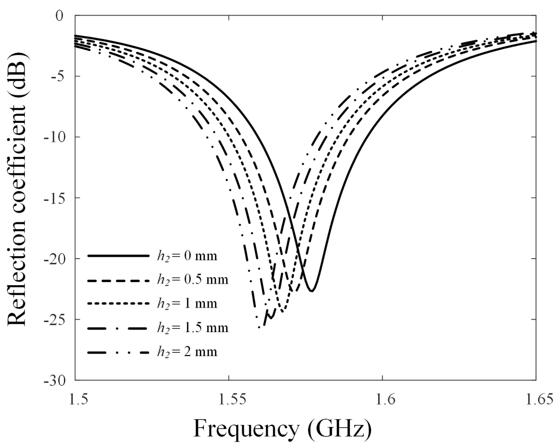

FIGURE 3. Reflection coefficients according to the variation of the superstrate height h_2 by the FEKO EM simulation software.

are infinite. Then, the derived results are compared with the data obtained from a commercial electromagnetic (EM) simulation software [27]. The proposed structure is further demonstrated by fabricating several superstrate modules with different thicknesses. The results confirm that the proposed structure provides the capability of frequency tuning with the maximum frequency shift of 20 MHz with maintaining the CP characteristic when the superstrate thickness is 2 mm. In addition, since the module is designed to affect only the

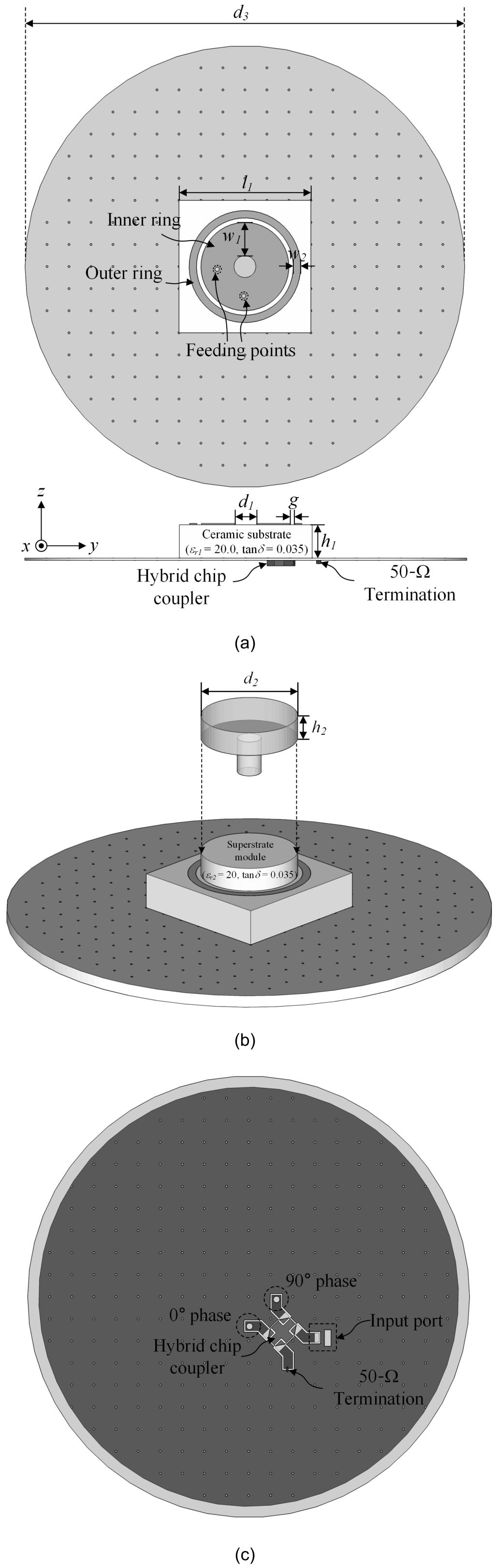

FIGURE 4. Geometry of the proposed antenna with the superstrate module. (a) Top and side view. (b) Isometric view with placing the superstrate module. (c) Bottom view.

TABLE 1. Design parameters of the proposed antenna.

Parameter	Value
l_1	50 mm
w_1	8 mm
w_2	0.6 mm
h_1	10 mm
h_2	0, 0.5, 2 mm
d_1	7.4 mm
d_2	23.4 mm
d_3	127 mm
g	0.4 mm

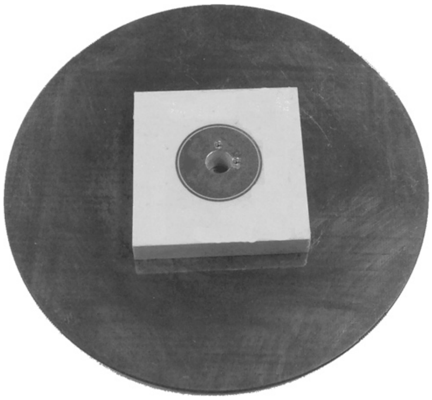

(a)

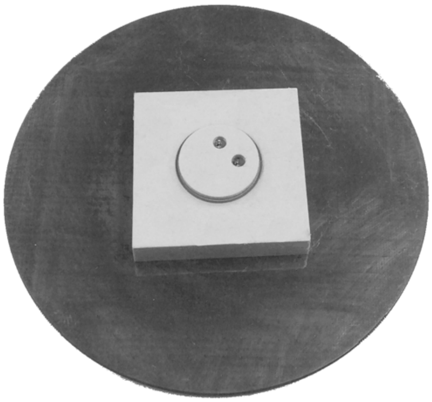

(b)

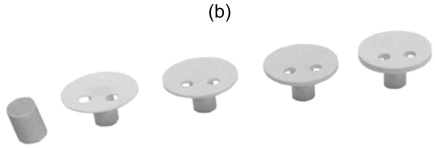

(c)

FIGURE 5. Photographs of the fabricated antenna. (a) The fabricated antenna without the superstrate module. (b) The fabricated antenna with the superstrate module. (c) The fabricated superstrate module with different head thicknesses.

upper resonance, the frequency interval between two resonances can also be adjusted by replacing the superstrate thickness.

II. THEORIOTICAL BACKGROUND

Fig. 1 illustrates a conceptual geometry of a circular patch antenna for radius a with an infinite superstrate, substrate,

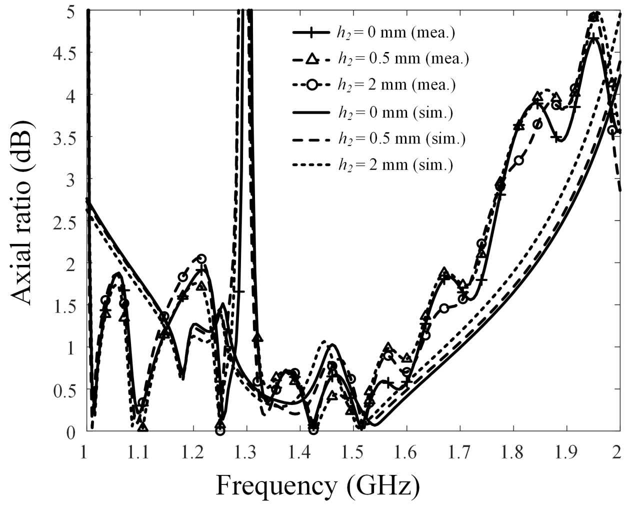

FIGURE 6. Measured axial ratios of the proposed antenna with different heights of the superstrate modules.

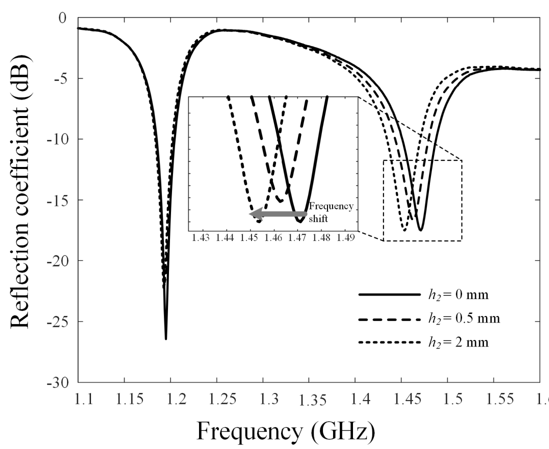

FIGURE 7. Measured reflection coefficients of the proposed antenna with different heights of the superstrate modules.

and the ground. The substrate and the superstrate have relative permittivity of ε_{r1} and ε_{r2} with heights of h_1 and h_2, respectively. In the past study, the resonant frequency $f_{r,min}$ of the circular patch antenna is formulated as

$$f_{r,nm} = \frac{\alpha_{nm} c_0}{2\pi a_{eff}\sqrt{\varepsilon_{eff}}}, \tag{1}$$

where α_{nm} is the m^{th} zero of the derivative of the Bessel function of order n, ε_{eff} is the effective permittivity of the patch antenna in the existence of the superstrate. The effective radius is denoted as a_{eff}, and c_0 is the velocity of light in free space [28]. The detailed expression for ε_{eff} was introduced in [29], which can be written as

$$\begin{aligned}\varepsilon_{eff} &= \varepsilon_{r1} p_1 + \varepsilon_{r1}(1-p_1)^2 \\ &\quad \times \left[\varepsilon_{r2}^2 p_2 p_3 + \varepsilon_{r2}\left\{p_2 p_4 + (p_3+p_4)^2\right\}\right] \\ &\quad \times \left[\begin{array}{l}\varepsilon_{r2}^2 p_2 p_3 p_4 + \varepsilon_{r1}(\varepsilon_{r2} p_3 + p_4)(1-p_1-p_4)^2 \\ + \varepsilon_{r2} p_4\left\{p_2 p_4 + (p_3+p_4)^2\right\}\end{array}\right]^{-1}\end{aligned} \tag{2}$$

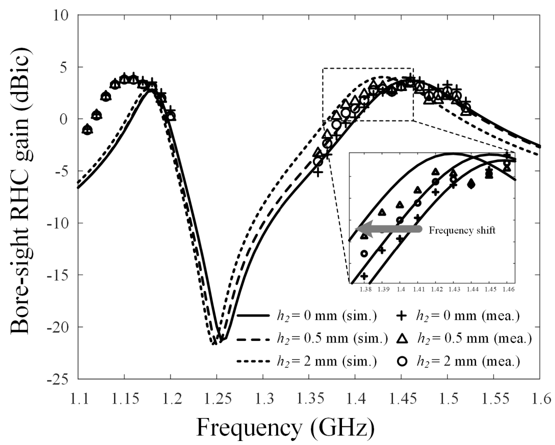

FIGURE 8. Bore-sight RHC gains of the proposed antenna with different heights of the superstrate modules.

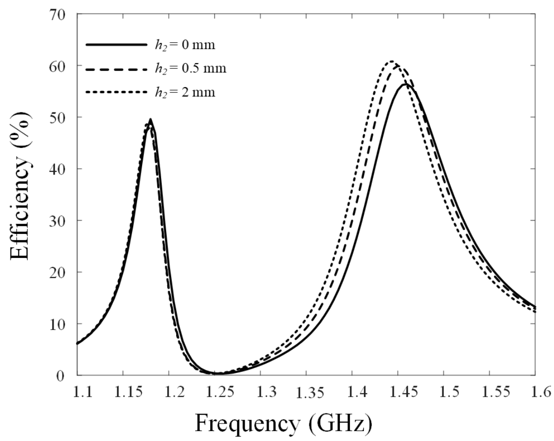

FIGURE 9. Efficiency of the proposed antenna with different heights of the superstrate modules.

The parameters p_1, p_2, p_3, and p_4 indicate relationships between the substrate and superstrate heights of h_1 and h_2 with the effective radius, and their definitions are presented in [29]. To make these equations be more feasible for the circular ring patch antenna, we modify the formula of the effective radius a_{eff} as

$$a_{eff} = a\sqrt{1+q} \quad (a = a_1/a_2)\,, \tag{3}$$

where a is the ratio between the inner radius a_1 and the outer radius a_2. In our approach, we use the ratio a to compute a_{eff} because the total field can be obtained from the superposition of the fields radiated by the inner and outer edges of the ring patch [30]. Substituting the calculated a_{eff} for (2) leads to ε_{eff} as a function of ε_{r2} and h_2, as shown in Fig. 2, when assuming $\varepsilon_{r1} = 20$ and $h_1 = 10$ mm. The dashed lines indicate the relative permittivity of some commercial materials such as FR-4 ($\varepsilon_{r2} = 4.4$), Cer-10 ($\varepsilon_{r2} = 10$), and Ceramic ($\varepsilon_{r2} = 20$). As can be observed, adjustments of h_2 and ε_{r2} result in different ε_{eff} that can tune $f_{r,min}$ without changing the shape of the physical antenna size. For example, ε_{eff} of the antenna with Cer-10 varies between 11 and 15.5 for h_2 from 0 mm to 40 mm, which gives the maximum adjustment of the resonant point $f_{r,min}$ by 17.1%.

TABLE 2. Antenna performance comparisons.

Design	Structure of the substrate layer	Operating frequency band	Frequency tuning technique	Overlapping bandwidth (GHz) [lower, upper (%)]	Max. gain (dBic)	Patch dimension (λ_0) in center frequency
[18]	Single	Wideband	–	9.03 – 11.12 21	12.5 (array)	1.1 × 1.1× 0.02
[19]	Stacked	Wideband	–	2.28 – 2.77 19.4	5.7	0.3× 0.3× 0.02
[20]	Stacked	Wideband	PIN diode	2.44 – 2.5 2.43	6	0.72× 0.72× 0.12
[21]	Stacked	Dual	–	2.25, 5.1, 5.4 –	7	0.21× 0.21× 0.02
[22]	Stacked	Dual	–	– 1.3, 1.1	5.2	0.21× 0.21× 0.02
[23]	Single	Dual	Air gap superstrate w/ parastic patch	– 1.1, 1.3	7	0.16× 0.16× 0.02
Proposed work	Single	Dual	Superstrate module	1.18 – 1.20, 1.44 – 1.47 1.51, 2.47	3.2	0.06× 0.06× 0.06

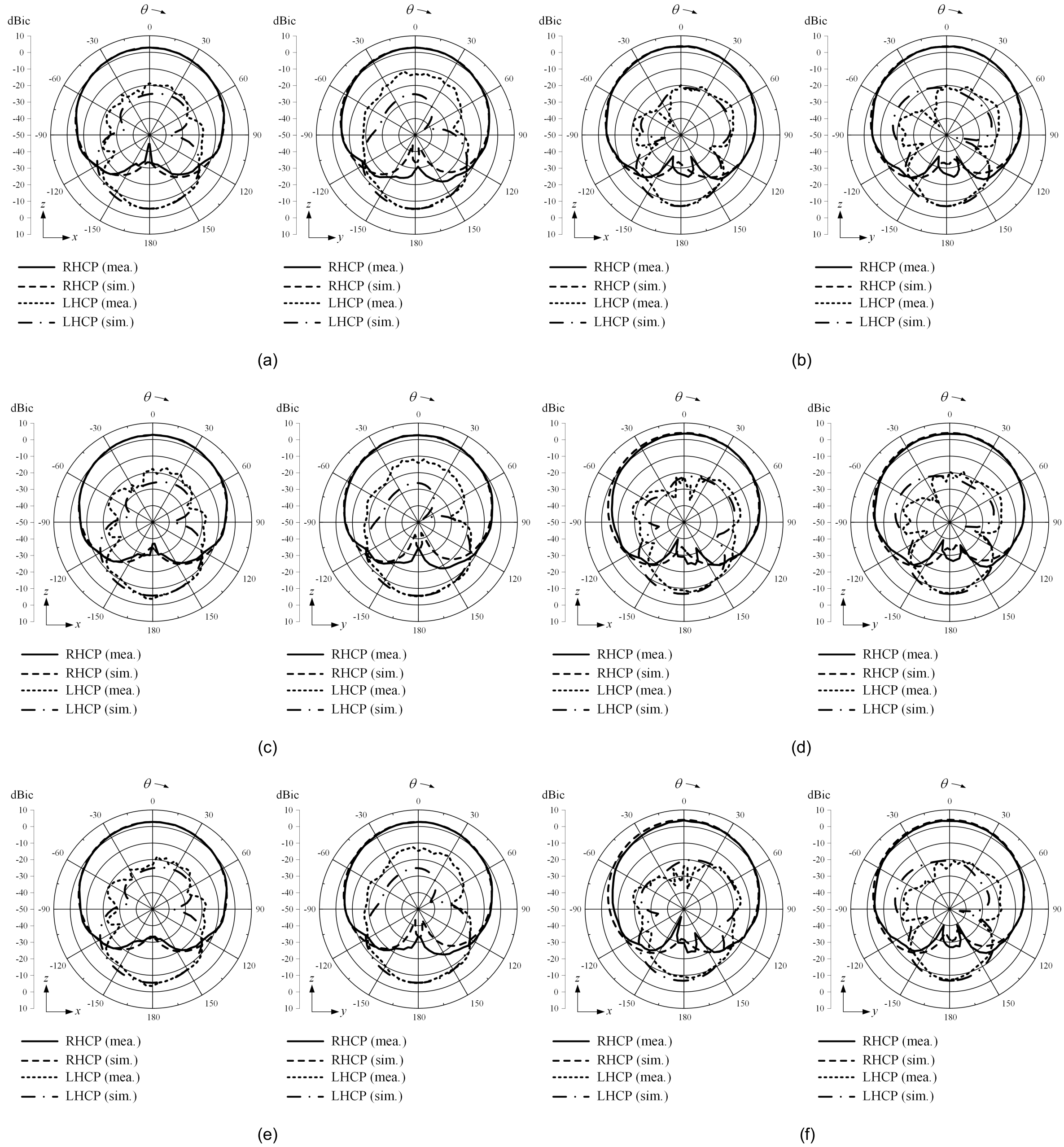

FIGURE 10. **Comparison of simulated and measured radiation patterns of RHC and LHC gains in *zx*- and *zy* - planes. (a) $h_2 = 0$ mm at 1.18 GHz. (b) $h_2 = 0.5$ mm at 1.18 GHz. (c) $h_2 = 2$ mm at 1.18 GHz. (d) $h_2 = 0$ mm at 1.42 GHz. (e) $h_2 = 0.5$ mm at 1.42 GHz. (f) $h_2 = 2$ mm at 1.42 GHz.**

To confirm the calculated results, we model the ring patch antenna with the infinite geometry using the FEKO EM Software. The antenna is designed by: inner and outer radii of 11.7 mm and 1.3 mm, $\varepsilon_{r1} = \varepsilon_{r2} = 20$, and $h_1 = 10$ mm. Fig. 3 shows simulated reflection coefficients as the superstrate height h_2 increases from 0 mm to 2 mm at an interval of 0.5 mm. As can be seen, the increment of h_2 shifts the resonance frequency toward lower bands with the maximum variation of 17 MHz, which covers the entire GPS L1 band (1563 MHz $\leq$ *frequency* $\leq$ 1587 MHz).

III. PROPOSED STRUCTURE AND MEASURED RESULTS

Fig. 4 shows the geometry of the single-layer dual-ring CP antenna with the superstrate module. The proposed antenna consists of inner and outer circular ring patches with widths of w_1 and w_2, respectively. The gap between two ring patches is g, which adjusts the dual-frequency band ratio [31], and the diameter of the cylindrical hole in the middle of the inner ring patch is designed by d_1. The head of the superstrate module has diameter d_2 and thickness h_2, and the antenna substrate has edge length l_1 with thickness h_1. For CP properties, the inner patch is fed by two pins of an external hybrid chip coupler (XC1400P-03S from Anaren) for the quadrature excitation [32], and the feeding network is embedded at the bottom of the printed circuit board (PCB). The PCB has diameter d_3 and is also used as the antenna ground. Note that, in our approach, the same dielectric properties of $\varepsilon_{r1} = \varepsilon_{r2} = 20$ and tan$\delta = 0.035$ are employed for both the superstrate module and the antenna substrate, and other design parameters are specified in Table 1.

Figs. 5(a) and 5(b) show photographs of the fabricated antenna without and with the superstrate model, and Fig. 5(c) presents fabricated superstrate modules with various thicknesses: $h_2 = 0$ mm, $h_2 = 0.5$ mm, $h_2 = 1$ mm, $h_2 = 1.5$ mm, and $h_2 = 2$ mm. These modules are designed to fit into the substrate hole so that the off-set error is minimized by aligning the center of the module with the antenna center.

Fig. 6 presents the measured and simulated AR as a function of frequency. The simulated data for different h_2 are specified by solid, dashed, and dotted lines, and those of the same lines with plus, circle and triangle markers indicate measured results. The tendency of the measured AR curve agrees well with that of the simulation, and the maximum difference is less than 1.3 dB within the 3-dB AR bandwidth, which is greater than 475 MHz for all h_2 values.

Fig. 7 presents the measured reflection coefficients of the fabricated antenna, and the solid, dashed, and dotted lines indicate results when $h_2 = 0$ mm, $h_2 = 0.5$ mm, and $h_2 = 2$ mm, respectively. As we aimed, the resonant frequency tends to shift toward the lower frequency band with the minimum values of −17.3 dB at 1.472 GHz ($h_2 = 0$ mm), −16.6 dB at 1.464 GHz ($h_2 = 0.5$ mm), and −17.5 dB at 1.452 GHz ($h_2 = 2$ mm). In addition, the lower resonance is not affected by the superstrate height because the alignment above the inner ring patch is firmly fixed to avoid overlapping the outer ring patch.

Fig. 8 shows variations of the measured and simulated bore-sight gains for the right-hand circular (RHC) polarization according to h_2. The simulated data for different h_2 are specified by solid, dashed, and dotted lines. Plus, circle, and triangle markers indicate measured results. Due to the resonance shift, the bore-sight gain also tends to shift toward the lower frequency band as h_2 increases. This implies that the gain can be further improved by exchanging the substrate module to compensate for the unexpected frequency shifts. For example, the measured gain at 1.42 GHz is 2.3 dBic without the superstrate, and this can be improved to 3.6 dBic by using the superstrate with $h_2 = 2$ mm, while the gain of the lower resonance maintains to be identical as 3.1 dBic at 1.18 GHz. To more interpret the CP characteristics, the overlapping bandwidth is calculated in the upper and lower frequency band, which means that the bandwidths are overlaid between the return-loss bandwidth and the axial ratio bandwidth of the CP antenna [18]–[20]. The overlapping bandwidths of 37 MHz (2.51 %), 36 MHz (2.46 %), and 36 MHz (2.47 %) are obtained in the upper frequency band with changing h_2 of 0 mm, 0.5 mm, and 2 mm although the minimum overlapping bandwidth of 20 MHz (1.51 %) is conserved in the lower band. We also compare the performances between the proposed antenna and the reference CP antennas, and the detailed explanations are specified in TABLE 2.

Fig. 9 illustrates that the proposed antenna maintains the efficiency of 49.1 % in the lower band despite of varying the superstrate height h_2, in contrast, the efficiency in the upper frequency band gradually increases from 56.4 % to 60.7 % as h_2 is changed from 0 mm to 2 mm. This result is due to the fact that the dielectric loss of the superstrate module does not affect the efficiency of the outer ring patch since the superstrate has the same diameter as the inner ring patch.

Fig. 10 shows measured radiation patterns for various h_2 values in comparison with the simulated data. We present patterns for both the RHC and left-hand circular (LHC) gains in *zx*- and *zy*- planes at 1.18 GHz and 1.42 GHz. In the bore-sight direction, the measured results of the cross-polarization levels are lower than −16 dB in both *zx*- and *zy*-planes at 1.18 GHz, and those at 1.42 GHz are maintained to be less than −23.2 dB in *zx*-plane and −22.9 dB in *zy*-plane without serious pattern distortions in the upper hemisphere.

IV. CONCLUSION

we have proposed the design of a single-layer dual-ring CP antenna using the mushroom-shaped superstrate module that can compensate for the unwanted frequency shift. The superstrate module was designed as the mushroom-shape in order to easily insert the exact center of the antenna to tune the resonant frequency, and the proposed antenna had inner and outer circular ring patch for the dual-band operation. As a verification process, we fabricated the proposed antenna and the superstrate modules with various heights. The maximum frequency shift was observed as 20 MHz with the improved gain of about 0.9 dB at 1.42 GHz. The AR values were below 3 dB in both upper and lower frequency band, and the cross-polarization levels of the fabricated antenna were less than −16 dB without pattern distortions despite of changing the height of superstrate module. These results demonstrate that the proposed antenna is suitable for tuning the unexpected frequency shift to enhance the gain without any distortions on the AR and the patterns.

REFERENCES

[1] D. Li, P. Guo, Q. Dai, and Y. Fu, "Broadband capacitively coupled stacked patch antenna for GNSS applications," *IEEE Antennas Wireless Propag. Lett.*, vol. 11, pp. 701–704, 2015.

[2] Nasimuddin, X. Qing, and Z. N. Chen, "A compact circularly polarized slotted patch antenna for GNSS applications," *IEEE Trans. Antennas Propag.*, vol. 62, no. 12, pp. 6506–6509, Dec. 2014. [Online]. Available: https://ieeexplore.ieee.org/author/37270712800

[3] F. Mariottini, M. Albani, E. Toniolo, D. Amatori, and S. Maci, "Design of a compact GPS and SDARS integrated antenna for automotive applications," *IEEE Antennas Wireless Propag. Lett.*, vol. 9, pp. 405–408, 2010.

[4] M. C. Kang, H. Choo, and G. Byun, "Design of a dual-band microstrip loop antenna with frequency-insensitive reactance variations for an extremely small array," *IEEE Trans. Antennas Propag.*, vol. 65, no. 6, pp. 2865–2873, Jun. 2017.

[5] J. Hur, H. Choo, and G. Byun, "Design of a small controlled reception pattern antenna array with a single-layer coupled feed structure for enhanced bore-sight gain and a matching bandwidth," *Electromagnetics* , vol. 37, no. 5, pp. 297–309, Jun. 2017.

[6] T. Lee, D.-H. Lee, H. Choo, and G. Byun, "A method of substrate shaping to improve gain of active-element pattern for small arrays," *IEEE Antennas Wireless Propag. Lett.*, vol. 16, pp. 1601–1604, 2017.
[7] J.-H. Lu and K.-L. Wong, "Slot-loaded, meandered rectangular microstrip antenna with compact dual frequency operation," *Electron. Lett.*, vol. 34, no. 11, pp. 1048–1050, May 1998.
[8] Y. Sung, "Size reduction technique for slot antenna," *Electron. Lett.*, vol. 49, no. 23, pp. 1425–1426, Nov. 2013.
[9] R. Li and S. Xiao, "Compact slotted semi-circular antenna for implantable medical devices," *Electron. Lett.*, vol. 50, no. 23, pp. 1675–1677, 2014.
[10] W.-I. Son, W.-G. Lim, M.-Q. Lee, S.-B. Min, and J.-W. Yu, "Design of compact quadruple inverted-F antenna with circular polarization for GPS receiver," *IEEE Trans. Antennas Propag.*, vol. 58, no. 5, pp. 1503–1510, May 2010.
[11] X. Zhang and L. Zhu, "Gain-enhanced patch antenna without enlarged size via loading of slot and shorting pins," *IEEE Trans. Antennas Propag.*, vol. 65, no. 11, pp. 5702–5709, Nov. 2017.
[12] R. Chair, C. L. Mak, K.-F. Lee, K.-M. Luk, and A. A. Kishk, "Miniature wide-band half U-slot and half E-shaped patch antennas," *IEEE Trans. Antennas Propag.*, vol. 53, no. 8, pp. 2645–2652, Aug. 2005.
[13] J. Anguera, E. Martnez-Ortigosa, C. Puente, C. Borja, and J. Soler, "Broadband triple-frequency microstrip patch radiator combining a dual-band modified Sierpinski fractal and a monoband antenna," *IEEE Trans. Antennas Propag.*, vol. 54, no. 11, pp. 3367–3373, Nov. 2006.
[14] J. P. Gianvittori and Y. Rahmat-Samii, "Fractal antennas: A novel antenna miniaturization technique, and applications," *IEEE Antennas Propag. Mag.*, vol. 44, no. 1, pp. 20–36, Feb. 2002.
[15] C. Puente, J. Romeu, R. Pous, X. Garcia, and F. Benitez, "Fractal multi-band antenna based on the Sierpinski gasket," *Electron. Lett.*, vol. 32, no. 1, pp. 1–2, Jan. 1996.
[16] G. Byun, H. Choo, and H. Ling, "Optimum placement of DF antenna elements for accurate DOA estimation in a harsh platform environment," *IEEE Trans. Antennas Propag.*, vol. 61, no. 9, pp. 4783–4791, Sep. 2013.
[17] D. Sun, W. Dou, and L. You, "Application of novel cavity-backed proximity-coupled microstrip patch antenna to design broadband conformal phased array," *IEEE Antennas Wireless Propag. Lett.*, vol. 9, pp. 1010–1013, 2010.
[18] K. L. Chung and A. S. Mohan, "A circularly polarized stacked electromagnetically coupled patch antenna," *IEEE Trans. Antennas Propag.*, vol. 52, no. 5, pp. 1365–1369, May 2004.
[19] K. L. Chung, "A wideband circularly polarized H-shaped patch antenna," *IEEE Trans. Antennas Propag.*, vol. 58, no. 10, pp. 3379–3383, Oct. 2004.
[20] K. L. Chung, Y. Li, and C. Zhang, "Broadband artistic antenna array composed of circularly-polarized Wang-shaped patch elements," *AEU-Int. J. Electron. Commun.*, vol. 74, pp. 116–122, Feb. 2017.
[21] K. L. Chung, S. Xie, Y. Li, R. Liu, S. Ji, and C. Zhang, "A circular-polarization reconfigurable Meng-shaped patch antenna," *IEEE Access*, vol. 6, pp. 51419–51428, 2018.
[22] S. Kumar, A. Sharma, B. K. Kanaujia, M. K. Khandelwal, and A. K. Gautam, "Single-feed circularly polarized stacked patch antenna with small-frequency ratio for dual-band wireless applications," *Int. J. Microw. Wireless Technol.*, vol. 8, no. 8, pp. 1207–1213, Apr. 2016.
[23] S. Kumar, A. Sharma, B. K. Kanaujia, M. K. khandelwal, and A. K. Gautam, "Dual-band stacked circularly polarized microstrip antenna for S and C band applications," *Int. J. Microw. Wireless Technol.*, vol. 8, no. 8, pp. 1215–1222, Apr. 2016.
[24] S. Kumar, B. K. Kanaujia, M. K. Khandelwal, and A. K. Gautam, "Single-feed superstrate loaded circularly polarized microstrip antenna for wireless applications," *Wireless Pers. Commun.*, vol. 92, no. 4, pp. 1333–1346, Feb. 2017.
[25] K. L. Lau, S. H. Wong, and K. M. Luk, "Wideband folded feed L-slot folded patch antenna," *IEEE Antennas Wireless Propag. Lett.*, vol. 8, pp. 340–343, 2008.
[26] C. A. Balanis, "Microstrip antennas," in *Antenna Theory and Design*, 3rd ed. Hoboken, NJ, USA: Wiley, 2005, pp. 816–819.
[27] Altair Engineering Inc. (2018).*FEKO EM Simulation Software*. [Online]. Available: http://www.altair.co.kr
[28] D. Guha, "Resonant frequency of circular microstrip antennas with and without air gaps," *IEEE Trans. Antennas Propag.*, vol. 49, no. 1, pp. 55–59, Jan. 2001.
[29] D. Guha and J. Y. Siddiqui, "Resonant frequency of circular microstrip antenna covered with dielectric superstrate," *IEEE Trans. Antennas Propag.*, vol. 51, no. 7, pp. 1649–1652, Jul. 2003.
[30] R. Garg, P. Bhartia, I. Bahl, and A. Ittipiboon, "Circular disk and ring antennas," in *Microstrip Antenna Design Handbook*, 1st ed. Norward, MA, USA: Artech House, 2001, pp. 317–398.
[31] T. Lee, H. Choo, B.-J. Jang, and G. Byun, "Design of single-layer microstrip antennas for dual-frequency-band ratio adjustment with circular polarization characteristics," *Electromagnetics*, vol. 37, no. 4, pp. 224–232, Jul. 2017.
[32] Anaren. (2012). *Model XC1400P-03S*. [Online]. Available: http://www.anaren.com

TAE HEUNG LIM received the B.S. and M.S. degrees in electronic and electrical engineering from Hongik University, Seoul, South Korea, in 2016 and 2018, respectively, where he is currently pursuing the Ph.D. degree in electronic and electrical engineering. His research interests include global positioning system antennas, time modulated array, antenna arrays, position optimization of array elements for adaptive beamforming, and wave propagations for radar applications.

HOSUNG CHOO (S'00–M'04–SM'11) received the B.S. degree in radio science and engineering from Hanyang University, Seoul, in 1998, and the M.S. and Ph.D. degrees in electrical and computer engineering from The University of Texas at Austin, in 2000 and 2003, respectively. In 2003, he joined the School of Electronic and Electrical Engineering, Hongik University, Seoul, South Korea, where he is currently a Professor. His current research interests include electrically small antennas for wireless communications, reader and tag antennas for RFID, on-glass and conformal antennas for vehicles and aircraft, and array antennas for GPS applications.

GANGIL BYUN (S'12–M'15) received the B.S. and M.S. degrees in electronic and electrical engineering from Hongik University, Seoul, South Korea, in 2010 and 2012, respectively, and the Ph.D. degree in electronics and computer engineering from Hanyang University, Seoul, in 2015. After his graduation, he returned to Hongik University to work as a Research Professor and performed active research for two years. He joined the Faculty of the Ulsan National Institute of Science and Technology, in 2018, where he is currently an Assistant Professor of electrical and computer engineering.

He has actively contributed to the consideration of both antenna characteristics and signal processing perspectives for the improvement of overall beamforming performances. His current research interests include the design and analysis of small antenna arrays for adaptive beamforming applications, such as direction of arrival estimation, interference mitigation, radar, circularly-polarized antennas, vehicular and aeronautic antennas, global positioning system antennas, and antenna and array configuration optimization.